Journal of Photochemistry and Photobiology A: Chemistry 205 (2009) 34–43

Contents lists available at ScienceDirect

Journal of Photochemistry and Photobiology A: Chemistry

journal homepage: www.elsevier.com/locate/jphotochem

Formal intramolecular photoredox reactions of phenylbenzophenone, xanthone and fluorenone methanols in aqueous solution

Devin Mitchell, Peter Wan*

Department of Chemistry, Box 3065, University of Victoria, Victoria, BC V8W 3V6, Canada

ARTICLE INFO

Article history:
Received 4 December 2008
Received in revised form 2 April 2009
Accepted 9 April 2009
Available online 18 April 2009

Keywords:
Benzophenone
Xanthone
Fluorenone
Photoredox
Acid catalysis
Photoenolization
Excited state proton transfer
Carbon acidity

ABSTRACT

To further explore the structural and chromophoric effects on the formal intramolecular photoredox reaction discovered in our laboratory for aromatic ketones such as benzophenone and anthraquinones in aqueous solution, we have investigated whether this photochemistry can be applied to xanthones, fluorenones, and benzophenones that are "extended" by a conjugated phenyl ring where the oxidizable group is distal to the benzophenone. It was found that 2-(hydroxymethyl)xanthone (**6**) exhibited sufficient photoactivity that the intramolecular photoredox reaction was observable under neutral conditions whereas 2-(hydroxymethyl)fluorenone (**7**) displayed only very low but clean photoreactivity in acid. The last feature of this study focuses on the extension of the electronic transmission from the carbonyl functional group to the benzylic alcohol, by insertion of an additional phenyl group, to give a biphenyl (phenylene) structural feature. The addition of the phenyl group gives rise to bichromophoric molecules (**8**–**10**) rather than monochromophoric substrates studied in the past. We find that the location of the hydroxymethyl substituent on the attached phenyl ring plays a pivotal role in the overall photobehaviour: only the *ortho*-substituted compound gave evidence of an intramolecular photoredox reaction, while the *meta*- and *para*-substituted compounds primarily exhibited photobehaviour that can be interpreted as an "aborted" intramolecular redox process. Overall, the results show that photoredox or related reaction can occur for all of these systems but added complexities make them less useful compared to what was observed for the "parent" benzophenone system.

1. Introduction

The photoreduction of benzophenone (**1**) was one of the first photoreactions described in the literature [1], but it took about 60 years before the mechanism was fully elucidated as arising via the triplet excited state [2,3]. Another well-known phenomenon of benzophenone (**1**) is that its triplet excited state is quenched by added acid, as first reported by Ledger and Porter [4]. Some 30 years later, Wirz and coworkers [5] established that protonation (at the carbonyl) of triplet benzophenone results in a remarkable overall *photohydration* reaction, to give water-adducts **2** and **3** with a preference for **2**, i.e., hydration at the *meta* position (Eq. (1)). This photoreaction of benzophenone in acid has remained undetected for over 60 years due most likely to the instability of the benzophenone hydration products, which readily revert back to **1**. Consistent with the proposed mechanism of photohydration, Wirz and coworkers [5] assigned a pK_a of −0.4 for the protonated triplet excited state, indicating that the carbonyl oxygen is much more basic in T_1 than the ground state.

It seems reasonable to assume that the facile protonation of triplet excited benzophenone (**1**) and related compounds might lead to other types of acid catalyzed photochemistry yet to be uncovered. Indeed, recently we reported photochemical reactions of benzophenones and related compounds that require water or acid catalysis, in which protonation (at carbonyl) of triplet aromatic ketones (acetophenone, benzophenone and anthraquinone) is formally required [6]. One of these reactions is the formal acid catalyzed intramolecular redox reaction of 3-(hydroxymethyl)benzophenone (**4**) to give **5** (Eq. (2)) [6c,d]. Notably, the *para* isomer is unreactive; the *ortho* isomer was not studied due to complications that would arise from the known competing intramolecular hydrogen abstraction pathway. The quantum efficiency is very high in acid (Φ = 0.6, pH 2). The reaction itself may be viewed as a formal transfer of electrons through the *meta* positions of the benzene ring, which cannot be accomplished in the ground state. Evidence that the reaction is an intramolecular process catalyzed by water/acid was provided by the observation that the reaction became cleaner with dilution, with no loss in efficiency. The proposed mechanism of reaction [6c,d] requires protonation of the triplet excited state (to give an excited triplet carbocation) in common with the proposed mechanism for the photohydration of benzophenone [5]. However, instead of overall hydration (attack by

* Corresponding author. Tel.: +1 250 721 8976; fax: +1 250 721 7147.
E-mail address: pwan@uvic.ca (P. Wan).

1010-6030/$ – see front matter © 2009 Elsevier B.V. All rights reserved.
doi:10.1016/j.jphotochem.2009.04.004

water on the cation), the appropriately located hydroxymethyl substituent provides a new reaction pathway leading to (remarkably) overall oxidation of this group (via benzylic C–H deprotonation) and reduction of the benzophenone ketone [6c,d]. Overall, one could summarize the reactivity as due to a type of charge transfer coupled with proton transfer mechanism. That is, excited state charge transfer to the benzophenone carbonyl is trapped by protonation at the carbonyl oxygen followed by deprotonation (another proton transfer) of the C–H of the CH_2OH moiety.

In this work, we report exploratory studies with an emphasis on structural changes that address two new aspects: (a) whether similar photochemistry can occur for related aromatic ketones such as xanthones and fluorenones (**6** and **7**, respectively) and (b) whether the photoredox reaction can be induced over a longer distance in several 3-phenyl-substituted benzophenones **8**–**10**. The results show that similar reaction can occur for these systems but added complexities make them less useful compared to the "parent" benzophenone system.

2. Experimental details

2.1. General

^{1}H NMR spectra were recorded on either a Bruker AC300 (300 MHz) or AVANCE 500 (500 MHz) instrument. Mass spectra were obtained on a Kratos Concept H (EI) instrument. UV–vis spectra were recorded on a Varian Cary 5 instrument. Infrared spectra were recorded on a PerkinElmer FTIR Spectrum 1000 using NaCl plates. Melting point values were obtained using a Gallenkamp apparatus. All solvents and common starting materials used for synthesis (ACS grade) were purchased from Aldrich Chemical Company and used as received unless otherwise noted. Organic extracts were dried over anhydrous magnesium sulfate and filtered. Deuterated solvents D_2O, $CDCl_3$ were purchased from Cambridge Isotope laboratory containing 99.9% D. D_2SO_4 was obtained Aldrich Chemical company and contained 99.9% D. Preparative TLC was carried out on 20 cm × 20 cm silica gel GF Uniplates (Analtech). The indicated "pH" of H_2O–CH_3CN solutions used in this study is that of the water portion, measured prior to combining with the CH_3CN portion. The pHs were adjusted using aq. H_2SO_4 as required.

2.2. Materials

2.2.1. 2-(Hydroxymethyl)xanthone (*6*)

Xanthone **6** was made from the corresponding 2-methylxanthone, a known compound [7], made via an Ulmann-type coupling procedure [7], mp 116–120 °C (lit. 122–123 °C [7]); ^{1}H NMR (300 MHz, $CDCl_3$) δ 8.33 (dd, 1H, 8.0 Hz, 1.4 Hz), 8.11 (d, 1H, 0.95 Hz), 7.70 (ddd, 1H, 1.4 Hz, 6.9 Hz, 6.9 Hz), 7.55–7.45 (m, 2H), 7.41–7.32 (m, 2H), 2.46 (s, 3H); ^{13}C NMR (125 MHz, $CDCl_3$) δ 177.55, 156.42, 154.63, 136.32, 134.87, 133.93, 126.96, 126.25, 123.93, 122.03, 121.69, 118.17, 117. 97, 21.07; MS (EI) *m*/*z*; 210 (100, M^+), 181, (40), 152 (10), 105 (10); HRMS, calculated for $C_{14}H_{10}O_2$ 210.0681; observed 210.0678. The synthesized 2-methylxanthone was then taken to **4** as follows: 2.30 g (10.9 mmol) of 2-methylxanthone was dissolved in 40 mL benzene. N-bromosuccinimide (2.34 g, 13.1 mmol) and benzoyl peroxide (0.010 g, 0.07 mmol) were added and the mixture refluxed overnight for 12 h under an atmosphere of N_2. The following day an off-white precipitate was visible. The precipitate was dissolved in 200 mL CH_2Cl_2 and washed twice with 100 mL distilled water before drying with anhydrous magnesium sulfate. Upon filtration and solvent removal, crude 2-(bromomethyl)xanthone was produced (crude yield 2.62 g). The crude product was dissolved in 75 mL dioxane and then calcium carbonate (5.53 g, 55.2 mmol) was added along with 75 mL distilled H_2O. This mixture was the reluxed overnight for 17 h. The solvent was removed using a rotary evaporater and the residue subsequently dissolved by alternately adding 1 M HCl and CH_2Cl_2 until all the solid had dissolved. The organic layer was removed and the aqueous layer was extracted three times with 50 mL CH_2Cl_2 until all the solid dissolved. The organic layers were combined, washed twice with 100 mL saturated sodium bicarbonate solution and dried with anhydrous magnesium sulfate. Filtration and solvent removal resulted in the crude product (1.11 g) in 45% yield (3:1 alcohol to aldehyde ratio). Recrystallization from ethanol resulted in the pure **4** (white needle-like crystals) in 10% overall yield, mp 140–145 °C; ^{1}H NMR (300 MHz, $CDCl_3$) δ 8.31 (dd, J = 1.4, 7.7 Hz, 1H), 8.26 (d, J = 1.8, 1H), 7.76–7.67 (m, 2H), 7.44–7.43 (m, 2H), 7.37 (t, J = 7.8, 1H), 4.80 (s, 2H); ^{13}C NMR (125 MHz, $CDCl_3$) δ 177.37, 156.30, 155.73, 136.98, 135.03, 134.05, 126.89, 124.79, 124.13, 121.90, 121.62, 118.48, 118.14, 64.62; IR (neat, NaCl plates): ν (cm^{-1}) 3367, 1659, 1608, 1488, 1467, 1320, 1243, 1207, 1139, 1015, 834, 760; UV–vis (1:1 H_2O–CH_3CN): λ_{max} (nm) 341 (ε13,000), 262 (ε26,000), 241 (ε91,000), 204 (ε38,000); MS (EI) *m*/*z*; 226(M^+, 80), 209 (20), 197 (100), 180 (15), 149 (50), 139 (25), 69 (30), 57 (30), 55 (30), 44 (30); HRMS, calculated for $C_{14}H_{10}O_3$ 226.0630; observed 226.0629.

2.2.2. 2-(Hydroxymethyl)fluorenone (*7*)

Compound **7** was obtained by selective BH_3 reduction of commercially available 9-fluorenone-2-carboxylic acid (Aldrich) according to the procedure of Brown and coworkers [8], mp 135–141 °C; ^{1}H NMR (300 MHz, $CDCl_3$) δ 7.64–7.60 (m, 2H), 7.51–7.44 (m, 4H), 7.30–7.25 (m, 1H) 4.70(s, 2H); ^{13}C NMR (125 MHz, $CDCl_3$) δ 193.96, 144.50, 144.04, 142.46, 134.97, 134.78, 134.59, 133.34, 129.27, 124.61, 123.09, 120.63, 120.54, 64.98; IR (neat, NaCl plates), ν (cm^{-1}) 3409, 1713, 1602, 1455, 1342, 1288, 1255, 1174, 1102, 1047, 989, 824, 760, 733; UV–vis (1:1 pH 2 H_2SO_4–CH_3CN), λ_{max} (nm) 252 (ε14,000), 260 (ε22,000), 298 (ε600); MS (EI) *m*/*z*; 210 (M^+, 95), 193 (20), 181 (100), 165 (10), 152 (70), 76 (10); HRMS, calculated for $C_{14}H_{10}O_2$ 210.0681; observed 210.0681.

2.2.3. 3-(Trofluoromethanesulfonyloxy)benzophenone (*12*)

3-Hydroxybenzophenone (**11**; Aldrich) (4.0 g, 20.2 mmol) was placed in a 500-mL 2-necked round bottom flask with 9.8 mL pyridine (120 mmol). The reaction mixture was cooled to 0 °C using an ice-bath. Trifluoromethanesulfonyl anhydride (10 g, 35 mmol) was added to 50 mL distilled CH_2Cl_2 in a pressure equalizing dropping funnel and added drop wise to the reaction mixture over 20 min. After addition, the reaction mixture was allowed to warm to room temperature where it was stirred for 4.5 h. The solution was then poured into 300 mL ice water and the mixture placed in a separatory funnel. The organic fraction was removed and the aqueous fraction extracted three times with 100 mL dichloromethane. The organic fractions were combined and then washed twice with 100 mL 1M HCl to remove any pyridine before drying with anhydrous magnesium sulfate. It was then filtered and the solvent removed under vacuum to give ~6 g of **12** (90%) which was used in the following step below without further purification, ^{1}H NMR (300 MHz, $CDCl_3$) δ 7.84–7.76 (m, 3H), 7.72–7.68 (m, 1H), 7.65–7.55 (m, 2H), 7.52–7.45 (m, 3H).

2.2.4. General procedure for suzuki coupling of *12* with methylphenylboronic acids

The appropriate methylphenylboronic acid (Aldrich) was dissolved in deoxygenated toluene with K_2CO_3 and **12** in a 2-necked round bottom flask. The reaction apparatus was flushed with N_2 for 10 min before adding $Pd(PPh_3)_4$ through a sidearm and then purging again with nitrogen for 10 min before starting to heat. The mixture was refluxed overnight (17 h) and left to cool. After cooling the mixture was passed through a celite plug before removing

solvent under vacuum. The crude residue was purified by column chromatography (silica, 1:1 ether/hexanes). Recrystallization if necessary was accomplished using toluene.

*2.2.4.1. 3-(2′-(Methyl)phenyl)benzophenone (**13**).* The coupled product was formed using the general procedure from 2-methylphenylboronic acid (2.95 g, 22 mmol) in 55 mL deoxygenated toluene, 4.54 g (32.8 mmol) K_2CO_3, **12** (4.17 g, 13.1 mmol) and $Pd(PPh_3)_4$ (0.37 g, 0.32 mmol). This gave a crude product yield of 2.33 g (65% yield). After recrystallization 0.85 g (3.1 mmol) of pure product (off-white solid) was formed (24% yield), ^{1}H NMR (300 MHz, $CDCl_3$) δ 7.87–7.72 (m, 4H), 7.61–7.43 (m, 5H), 7.31–7.21 (m, 4H), 2.28 (s, 3H).

*2.2.4.2. 3-(3′-(Methyl)phenyl)benzophenone (**14**).* The coupled product was formed using the general procedure from 3-methylphenylboronic acid (4.13 g, 30.4 mmol) in 200 mL deoxygenated toluene, 5 g (36.2 mmol) K_2CO_3, **12** (~3 g, ~9 mmol) and $Pd(PPh_3)_4$ (0.58 g, 0.5 mmol). This gave an overall yield of 0.054 g (2% yield) after column chromatography (silica, 2:3 ether/hexanes), ^{1}H NMR (300 MHz, $CDCl_3$) δ 8.03–8.00 (m, 1H), 7.87–7.72 (m, 4H), 7.63–7.30 (m, 7H), 7.22–7.16 (m, 1H), 2.42 (s, 3H).

*2.2.4.3. 3-(4′-(Methyl)phenyl)benzophenone (**15**).* The coupled product was formed using the general procedure from 4-methylphenylboronic acid (8.20 g, 60.3 mmol) in 200 mL deoxygenated toluene, 10 g (72.4 mmol) K_2CO_3, **12** (~6 g, ~19 mmol) and $Pd(PPh_3)_4$ (0.58 g, 0.5 mmol). This gave a crude product yield of 4 g (25% yield). After recrystallization 0.50 g (1.8 mmol) of pure product was formed (7.4% overall yield), ^{1}H NMR (300 MHz, $CDCl_3$) δ 8.00 (s, 1H), 7.86–7.68 (m, 4H), 7.63–7.43 (m, 7H), 7.28–7.25 (m, 1H), 2.39 (s, 3H).

*2.2.5. General procedure for the bromination and hydrolysis of **13**–**15***

In a round bottom flash, the appropriate 3-(methylphenyl)benzophenone **13**–**15** was combined 1.3 molar equivalents of N-bromosuccinimide and catalytic amounts of benzoyl peroxide in benzene and refluxed under nitrogen overnight (17–19 h). After reaction the mixture was cooled to room temperature and the solution was washed twice with 50 mL distilled water to remove any remaining succinimide side product. The organic layer was then dried with anhydrous magnesium sulfate before filtering and removing the solvent under vacuum. The crude brominated compound was used directly in the hydrolysis step by dissolving the residue in dioxane and adding the equivalent amount of water plus 5 molar equivalents of $CaCO_3$. This mixture was then refluxed for 20 h and allowed to cool to room temperature. The solvent was removed under vacuum and enough dichloromethane and 1 M HCl was added until all of the solid residue had dissolved. The organic layer was collected and the aqueous layer extracted twice with dichloromethane before combining the organic layers. The combined organic layers were then washed twice with saturated sodium bicarbonate solution before drying with anhydrous magnesium sulfate. The mixture was then filtered and the solvent removed under vacuum. The resulting crude product was purified chromatographically (silica, 1:1 ether/hexanes).

*2.2.5.1. 3-(2′-(Hydroxymethyl)phenyl)benzophenone (**8**).* 3-(2′-Methylphenyl)benzophenone (**13**) (0.85 g, 3.1 mmol), N-bromosuccinimide (0.81 g, 4.6 mmol), benzoyl peroxide (0.012 g, 0.087 mmol) and 25 mL benzene were combined together according to the general synthesis to produce the brominated compound (1.01 g crude yield). This was used directly in the hydrolysis reaction by combining the crude brominated compound with 25 mL dioxane, 25 mL distilled water and 1.54 g (15.4 mmol) $CaCO_3$ and refluxing for 17 h. After workup a crude yield of 0.419 g (47% yield) was obtained. After column purification 0.179 g (20% yield) was obtained, ^{1}H NMR (500 MHz, $CDCl_3$) δ 7.84–7.78 (m, 4H), 7.63–7.58 (m, 1H), 7.58–7.52 (m, 3H), 7.49–7.45 (m, 2H), 7.40 (ddd, 7.4 Hz, 7.4 Hz, 1.5 Hz, 1H), 7.36 (ddd, 7.4 Hz, 7.4 Hz, 1.5 Hz, 1H), 7.29 (dd, 7.4 Hz, 1.5 Hz, 1H) 4.62 (s, 2H); ^{13}C NMR (125 MHz, $CDCl_3$) δ 196.79, 141.06, 140.54, 138.23, 137.91, 137.74, 133.37, 132.75, 130.87, 130.33, 130.29, 129.17, 128.83, 128.57, 128.51, 128.51, 128.42, 128.10, 63.32; IR (thin film, NaCl plates): ν (cm^{-1}) 3433, 3059, 3027, 2928, 2877, 1660, 1644, 1596, 1574, 1470, 1446, 1417, 1319, 1193, 1179, 1026, 948, 914, 820, 646; UV–vis (1:1 pH 2 H_2SO_4–CH_3CN): λ_{max} (nm) 253 (ε210,000); MS (EI) *m*/*z*; 288 (M^+, 30), 279 (30), 181 (20), 167 (40), 149 (100), 105 (85); HRMS, calculated for $C_{20}H_{16}O_2$ 288.1150; observed 288.1158.

*2.2.5.2. 3-(3′-(Hydroxymethyl)phenyl)benzophenone (**9**).* 3-(3′-Methylphenyl)benzophenone (**14**) (0.0540 g, 0.198 mmol), N-bromosuccinimide (1.88 g, 11 mmol), benzoyl peroxide (0.013 g, 0.094 mmol) and 40 mL benzene were combined together according to the general synthesis (see above) to produce the brominated compound (2.22 g crude yield). This was then used directly in the hydrolysis reaction by combining the crude brominated compound with 70 mL dioxane, 70 mL distilled water and 3.11 g (31 mmol) $CaCO_3$ and refluxing for 17 h. After workup a crude yield of 0.0238 g (40% yield) was obtained. After column purification 0.0076 g (14% yield) was obtained, ^{1}H NMR (300 MHz, $CDCl_3$) δ 8.00 (s, 1H), 7.87–7.72 (m, 4H), 7.63–7.33 (m, 8H), 4.75 (s, 2H), 1.93 (s, 1H); ^{13}C NMR (125 MHz, $CDCl_3$) δ 196.95, 141.82, 141.43, 140.71, 138.42, 137.75, 132.80, 131.30, 130.34, 129.40, 129.28, 128.97, 128.79, 128.59, 126.74, 126.58, 126.03, 65.47; IR (thin film, NaCl plates): ν (cm^{-1}) 3412, 3059, 3028, 2920, 2871, 1655, 1595, 1576, 1446, 1405, 1320, 1263, 1178, 1026, 1000, 964, 781; UV–vis (1:1 pH 2 H_2SO_4–CH_3CN) λ_{max} (nm) 202 (ε45,000), 249 (ε180,000); MS (EI) *m*/*z* 288 (M^+, 100), 211 (60), 182 (10), 165 (10), 152 (25), 105 (70), 77 (45), 51 (10); HRMS, calculated for $C_{20}H_{16}O_2$ 288.1150; observed 288.1159.

*2.2.5.3. 3-(4′-(Hydroxymethyl)phenyl)benzophenone (**10**).* 3-(4′-Methylphenyl)benzophenone (**15**) (0.50 g, 1.8 mmol), N-bromosuccinimide (0.43 g, 2.4 mmol), benzoyl peroxide (0.02 g, 0.14 mmol) and 40 mL benzene were combined together according to the general synthesis (see above) to produce the crude brominated compound (0.50 g (1.4 mmol) crude yield). This was used directly in the hydrolysis reaction by combining the crude brominated compound with 30 mL dioxane, 30 mL distilled water and 0.72 g (7.2 mmol) $CaCO_3$ and refluxed for 20 h. After workup a crude yield of 0.28 g (55%) was obtained. After column purification a colourless oil in a yield of 0.16 g (32% yield) was obtained, ^{1}H NMR (300 MHz, $CDCl_3$) δ 8.01–7.99 (m, 1H), 7.85–7.71 (m, 4H), 7.62–7.39 (m, 8H), 4.72 (s, 2H); ^{13}C NMR (125 MHz, $CDCl_3$) δ 196.95, 141.25, 140.72, 139.71, 138.41, 137.74, 132.79, 131.20, 130.34, 129.21, 128.98, 128.73, 128.58, 127.77, 127.60, 65.21; IR (thin film, NaCl plates): ν (cm^{-1}) 3400, 3059, 3027, 2920, 2871, 1656, 1651, 1595, 1579, 1446, 1434, 1319, 1253, 1014, 955, 813; UV–vis (1:1 pH 2 H_2SO_4–CH_3CN): λ_{max} (nm) 253 (ε200,000); MS (EI) *m*/*z*; 288 (M^+, 85), 211 (40), 182 (10), 165 (10), 152 (45), 105 (100), 77 (65), 55 (20); HRMS, calculated for $C_{20}H_{16}O_2$ 288.1150; observed 288.1152.

2.3. Product studies

2.3.1. General

All photolysis reactions were performed using a Rayonet RPR 100 photochemical reactor with 300 nm lamps and a water-cooled cold finger (ca. 15 °C). Solutions of substrate (~10^{-4} M, 150–300 mL) were photolyzed for times ranging from 1 to 120 min. The quartz photolysis tubes were purged with argon for 15 min prior to pho-

tolysis and then purged continuously with argon (unless otherwise noted) during photolysis. After photolysis of aqueous samples, the photolysis mixture was placed in a separatory funnel and extracted twice with dichloromethane (100 mL). The organic fractions were combined and dried over anhydrous magnesium sulfate before filtering and removing the solvent under vacuum. The residue was placed on a vacuum line for 15 min to remove any remaining solvent before characterization of the product mixture via NMR spectroscopy.

*2.3.2. Photolysis of **6***

Using a 500-mL quartz photolysis tube, **6** (10.7 mg) was dissolved in 150 mL CH_3CN and then 150 mL H_2O (neutral unbuffered) was added to give a concentration of 1.6×10^{-4} M. After photolysis at 300 nm (2 lamps) for 2 min, the solution was worked up analyzed by NMR, which gave a conversion of 5% of **16** with 2% **19** and about 10% oligomeric products. Photolysis for 10 min with 8 lamps using the same concentration resulted in essentially quantitative conversion and the products were separated by prep. TLC yielded **19**, ^{1}H NMR (300 MHz, $CDCl_3$) δ 9.98 (s, 1H), 8.35–8.29 (m, 3H), 8.09–8.07 (m, 2H), 7.92–7.90 (m, 1H), 7.79–7.61 (m, 3H), 7.50–7.40 (m, 3H), 7.40–7.35 (m, 2H), 6.00 (s, 1H), 4.30 (m, 2H) and **16**, ^{1}H NMR (300 MHz, $CDCl_3$) δ 10.10 (s, 1H), 8.81 (s, 1H), 8.39–8.22 (m, 2H), 7.80–7.68 (m, 2H), 7.60 (d, 1H), 7.40 (m, 1H), the latter being identical to an authentic sample.

*2.3.3. Photolysis of **7***

Using a 500-mL quartz photolysis tube, **7** (5 mg) was dissolved in 75 mL CH_3CN and 75 mL aq. H_2SO_4 (pH 2) was added to give a concentration of 1.6×10^{-4} M. Photolysis was carried out at 300 nm (16 lamps). At 15 min irradiation, essentially no reaction was observed. However, at 60 min photolysis, products **20** (10%) and **21** (10%) were observed. Fluorenone **21** was identified by comparison to the published NMR spectrum [9]. The proportion of fluorenone **20** was deduced based on NMR of the mixture containing both **20** and **21**. Thus characteristic of redox product **20** is the presence of a new aldehyde peak at δ 10.01 and a new methine proton at δ 5.65 as well as new isolated "singlet" in the aromatic region (δ 8.13) assignable to position 1 (between the reduced alcohol and the new aldehyde substituent). Moreover, photolysis in D_2O (pD 2) resulted in absence of the methine peak at δ 5.65 (but no changes in the other peaks) consistent with deuterium incorporation at this position as observed in previously reported photoredox reactions [6].

*2.3.4. Photolysis of **8***

Using a 500-mL quartz photolysis tube, **8** (14 mg) was dissolved in 150 mL CH_3CN and then 150 mL H_2O (pH 2) was added to give a concentration of 1.6×10^{-4} M. After photolysis at 300 nm for 5 min, the reaction was worked up and analyzed by ^{1}H NMR, which gave **22** (20%) and **23** (5%) and a trace of oligomeric products. The products were separated by prep TLC (silica, CH_2Cl_2), **22**, ^{1}H NMR (500 MHz, $CDCl_3$) δ 8.08 (s, 1H), 7.84–7.81 (m, 2H), 7.75–7.71 (m, 2H), 7.70–7.66 (m, 2H), 7.62–7.59 (m, 1H), 7.52–7.48 (m, 2H), 7.41 (ddd, 7.4 Hz, 7.7 Hz, 1.1 Hz, 1H), 7.36 (ddd, 7.4 Hz, 7.3 Hz, 1.2 Hz, 1H), 5.66 (s, 1H); ^{13}C NMR ($CDCl_3$, 125 MHz) δ 196.84, 150.01, 145.87, 140.67, 139.33, 138.91, 137.91, 132.79, 130.33, 130.30, 129.66, 128.75, 128.60, 125.47, 125.07, 121.55, 120.75, 75.35 (s); MS (EI) *m/z*; 286 (85, M^+), 207 (25), 181 (100), 152 (30), 105 (100); **23**, ^{1}H NMR (500 MHz, $CDCl_3$) δ 10.01 (s, 1H), 8.02 (dd, 7.7 Hz, 1.4 Hz, 1H), 7.86 (ddd, 4.5 Hz, 4.4 Hz, 1.8 Hz, 1H), 7.84–7.80 (m, 3H), 7.65 (ddd, 7.6 Hz, 7.4 Hz, 1.4 Hz, 1H), 7.61–7.57 (m, 3H), 7.54–7.43 (m, 4H); ^{13}C NMR ($CDCl_3$, 125 MHz) δ 196.40, 191.96, 144.90, 138.37, 138.16, 137.49, 134.04, 133.96, 132.94, 131.40, 131.10, 130.27, 129.92, 128.66, 128.53, 128.31.

*2.3.5. Photolysis of **9** and **10***

In a similar manner as for photolysis of **8** (pH 2), photolysis of both **9** and **10** yielded only the corresponding aldehydes **24** and **25** (along with oligomeric material), which were readily identified by comparison to authentic samples made during the synthesis of **8** and **9** (Scheme 1). Notably formation of **24** and **25** was absent when neutral solution was used.

2.4. Quantum yields of reaction

Quantum yields of reaction were estimated using the reported quantum yield for photoredox reaction of the parent benzophenone system **4** (Φ = 0.6 in pH 2) [6c]. Parallel solutions of compound and **4** at the same substrate concentration were photolyzed in a Rayonet reactor and the conversions (yields) were calculated by NMR.

2.5. UV–vis studies

Studies were carried using 3.0 mL quartz cuvettes. Stock solutions of the substrates were prepared in CH_3CN and 1–30 μL of this solution was injected into the stock using a syringe needle to give concentrations in the range 10^{-6} to 10^{-5} M. After purging with a stream of argon using a septum, the cuvettes were irradiated in a merry-go-round apparatus inside a Rayonet photochemical reactor.

3. Results and discussion

3.1. UV–vis and product studies

Initial product studies were carried out with xanthone **6** in pH 2 since the parent photoredox reaction of **4** was observed only below pH 3. Photolysis of **6** resulted in very efficient loss of substrate ($\Phi \sim 0.9$), comparable to the quantum yield for photoredox reaction of **4** itself. However, unlike **4**, the only photoproduct isolated from 6 is the corresponding *oxidized* xanthone aldehyde **16** at all conversions (Eq. (3), with no evidence for formation of the expected simple redox product **17**. We were originally perplexed at this finding since oxygen was excluded in much the same way as in the photolysis of **4**, which gave essentially quantitative conversion to the corresponding redox product **5** (Eq. (2)) without evidence for significant photooxidation. It became obvious, however, that if the simple redox product **17** was formed in pH 2, it would not be thermally stable since xanthenols are known to ionize to the corresponding ground state aromatic carbocation (i.e., **18**), with estimated $pK_{R+} \sim 1$ [10]. Moreover, reasonably stable carbocations of the type **18** are known to undergo disproportionation (via hydride transfer mechanism) with starting alcohols, to give a mixture of oxidized (i.e., **16**) and reduced products (Eq. (4)). This gave a reasonable (but not exhaustive) explanation for the lack of simple redox product observed on photolysis of **6** at pH 2.

The enhanced photoreactivity of **6** suggested that it might be reactive in neutral solution where the formation of **17** (and resulting side chemistry) would be avoided. To date, no simple benzophenone derivative has been found to undergo the intramolecular photoredox reaction in neutral solution [6]. Examination of the UV–vis traces observed on photolysis of **6** in neutral solution (~pH 7) indicated a highly reactive compound ($\Phi \sim 0.3$) (Fig. 1). Initial photolysis shows rapid loss of the strong 240 nm band assignable to the xanthone chromophore inherent in **6** without the formation of a weaker red-shifted band at 250 nm until at higher conversion. Examination of the peak at 290 nm also revealed a similar multistep wise transformation. Initial growth of the band at 290 nm was followed by a decrease after 1 min photolysis whereas the other bands continued the expected trends. These observations and the fact that clean isosbestic points were lacking indicate that the transformations involve formation of more than one product. Thus,

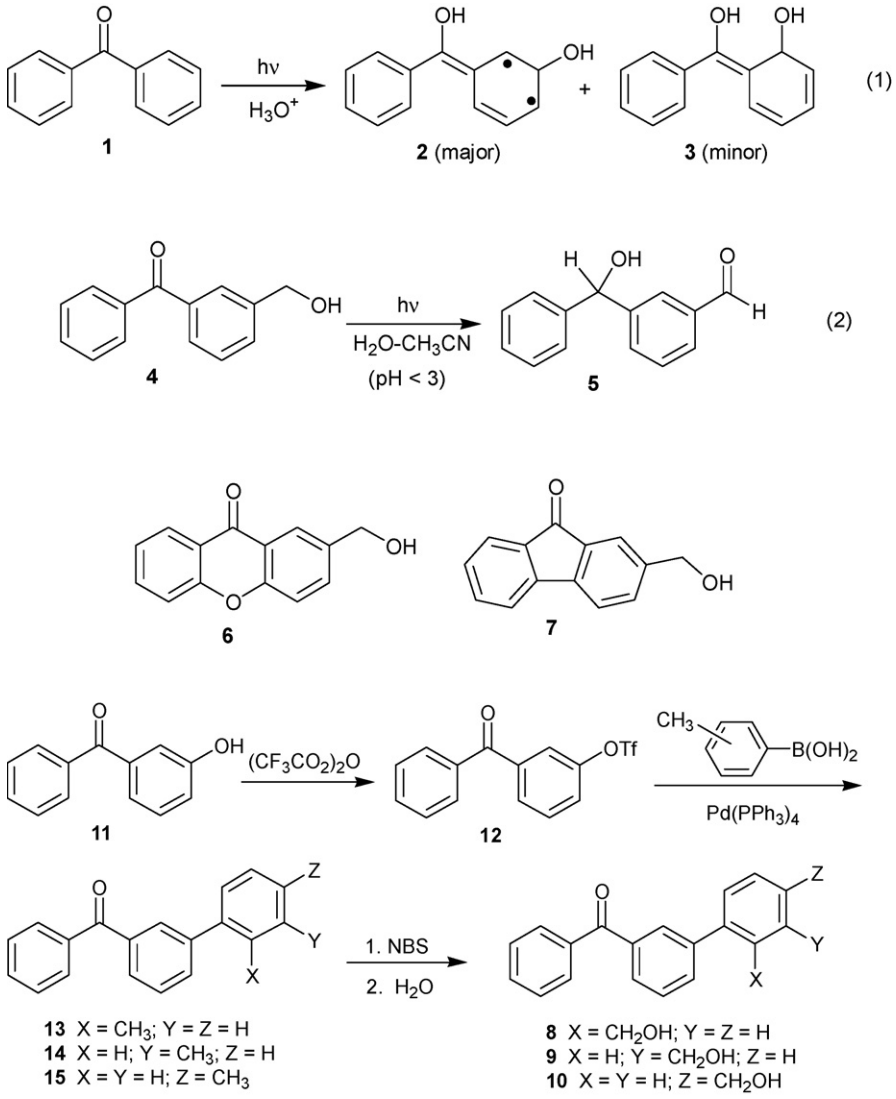

Scheme 1.

although the final trace observed resembles that of authentic **16**, its mechanism of formation is evidently more complex and involves more than one step. This is further confirmed in product studies followed by NMR below.

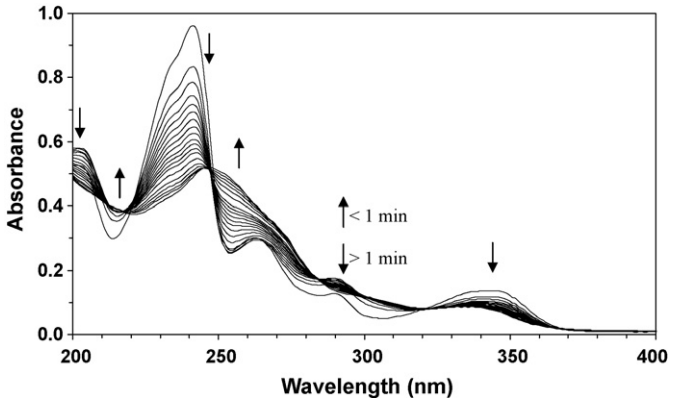

Fig. 1. UV–vis traces observed on photolysis of **6** in 1:1 H_2O–CH_3CN (λ_{ex} 300 nm). Initial traces were taken every 15 s with latter traces after 1–2 min. The final trace is consistent with the UV–vis spectrum of authentic **16**.

Photolysis of **6** in 1:1 H_2O–CH_3CN (neutral water) gave a mixture of **16** and the adduct **19** (Eq. (5)), with **19** dominating at low conversions. At higher conversions, **16** dominates. In addition, independent photolysis of **19** gave only **16** supporting the notion that **16** arises via secondary photochemistry of the initially formed adduct **19**, although the mechanism for this transformation requires formal oxidation of the benzylic ether link between the two xanthenyl chromophores. Photochemical reaction with residual oxygen in the solvent system cannot be excluded. Notably, thermal decomposition of **19** gave an equimolar mixture of **6** and **16** confirming at least the condensed structure of two xanthenes. Isolation of **19** is consistent with compound **6** having undergone a photoredox reaction to give the expected **17**, which is subsequently efficiently trapped by substrate catalyzed by trace acid (via **18**) to give **19** (Eq. (6)). We were surprised by the efficiency of this condensation reaction as under no circumstances were we able to isolate **17** as a discrete product. In any event, these results show that the xanthone system is very reactive with respect to intramolecular photoredox reaction although the process is not clean and is dominated by subsequent thermal and secondary photochemistry.

Initial semi-preparatory photolysis of the fluorenone derivative **7** under conditions employed for **4** and **6** (∼ pH 7 and 2) that would have given significant conversion resulted in no evidence of any

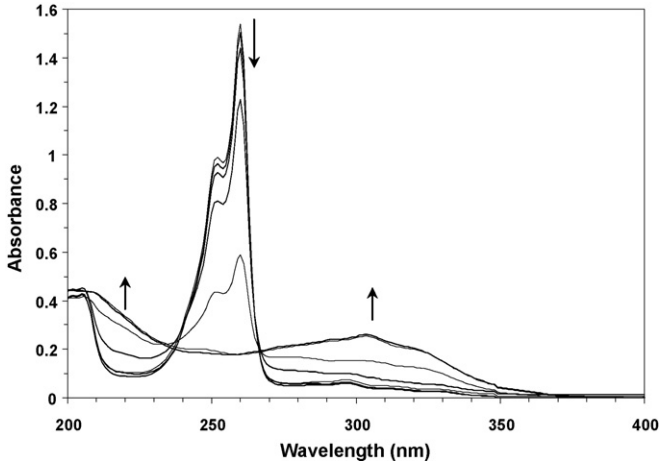

Fig. 2. UV–vis spectral traces observed on photolysis of **7** in 1:1 H_2O–CH_3CN (pH 2, λ_{ex} 300 nm). Initial traces were taken after 5 min irradiation to a maximum of 30 min irradiation at higher conversions. The final trace is consistent with a fluorene (not fluorenone) chromophore.

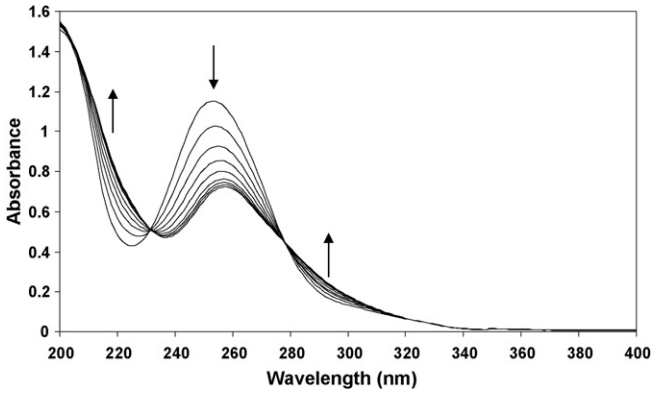

Fig. 3. UV–vis spectral traces observed on photolysis of **8** in 1:1 H_2O–CH_3CN (pH 2, λ_{ex} 300 nm). Traces taken after 30–60 s intervals.

photoreaction and the substrate could be recovered unchanged. Consequently, the reaction was followed using UV–vis since dilute conditions could be employed in addition to the enhanced sensitivity of the method. At pH 7, consistent the above runs, photolysis showed no changes in the UV–vis spectrum even on extended photolysis (up to 40 min), indicative of a very unreactive system. However, photolysis at pH 2 showed a slow but clean transformation (Fig. 2) showing significant loss of the intense 260 nm band associated with the conjugated fluorenone ketone, and the formation of a weaker and red-shifted band at 305 nm consistent with a simple fluorene chromophore (i.e., lacking the ketone). This suggests that photoredox chemistry may be occurring but with a very low efficiency. Subsequently, extended photolysis (up to 60 min, $\Phi < 0.001$) of **7** indeed gave a mixture of expected redox products **20** and **21** each in about 10% yield. Under no circumstances could **20** be observed without **21**. However, unlike the xanthone system **6**, this system was free of a condensation product (e.g., **19**) consistent with expected low reactivity of the 9-fluorenyl system of **20** to undergo ionization, which would in this case give the corresponding ground state *antiaromatic* 9-fluorenyl cation.

Initial UV–vis studies of the photolysis of extended benzophenone systems **8**–**10** in neutral solution (∼pH 7) and in pH 2 also provided valuable data. In all three systems, photolysis at pH 7 resulted in little if any change in the UV–vis absorption except on extended photolysis. However, photolysis at pH 2 gave smooth changes in UV–vis absorption. For example, for the *ortho* hydroxymethyl-substituted system **8** (Fig. 3), the UV–vis changes are characterized by reasonable isosbestic points and loss of the main 260 nm band with concomitant increase of a 310-nm band, suggestive of formation of a single or major photoproduct.

However, semi-preparatory photolysis of **8** at pH 2 did not result in a simple photoredox reaction but formation of a ketofluorenol **22** (50%, $\Phi \sim 0.2$) and oxidized product **23** (5%) (Eq. (8)). Ketofluorenol **22** is characterized (^{1}H NMR) by its distinctive benzhydrol methine at δ 5.66 and the better resolved aromatic protons on the fluorene ring due to the more rigid ring system. In contrast, photolysis of both **9** and **10** (isomers in which the CH_2OH group is too far away to interact with the adjacent phenyl ring) gave only the formally "oxidized" aldehyde products **24** and **25**, respectively (10–15% yield). Notably, these products are formed favourably only in pH 2 and lower (but not in neutral solution or in organic solvents) indicating that they are not simple oxidation products on reaction with residual oxygen. Extended photolysis of these two compounds or photolysis at higher substrate concentrations gave increasingly larger amounts of oligomeric products due to photoreduction pathways via bimolecular hydrogen abstraction by the benzophenone ketone (formation of broad NMR peaks in the δ 7.0–7.3 region assignable to unconjugated phenyl rings).

3.2. Mechanisms of reaction

It is clear from the product studies for the systems studied in this work that a simple photoredox reaction was not observed for any of the compounds, unlike that reported for the parent benzophenone **4**. Even for **4**, considerable care had to taken to carry out the reaction at low substrate concentration to prevent bimolecular hydrogen abstraction that results in formation of oligomeric products [6c,d]. However, all of the compounds studied reacted in aqueous solution (neutral or acidic) via pathways that could be ascribed to either an initial photoredox pathway or a "diverted" or an "aborted" one (vide infra). These pathways represent new chemistry for these aromatic ketones. Due to the complexity of the mechanistic pathways involved, we have not been able to shed any additional insights using nanosecond laser flash photolysis: only the corresponding triplet–triplet absorptions could be readily detected. Thus, the following discussion on reaction mechanisms is based on what we believe are reasonable structural transformations, knowing now what is possible for benzophenones **1** and **4** in aqueous acid, and also some qualitative theoretical calculations (vide infra).

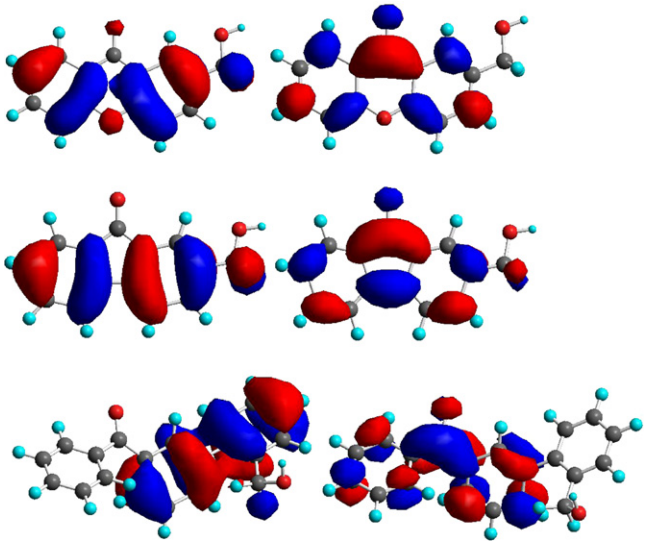

Fig. 4. Calculated HOMO (left) and LUMO (right) (Chem 3D, MOPAC/AM1) for **6** (top), **7** (center) and **8** (bottom).

First, it is instructive to examine HOMOs and LUMOs of the compounds studied in this work (Fig. 4) (Chem 3D, MOPAC/AM1) since similar calculations for the parent benzophenone system **4** have provided insights into their photoredox reactivity [6c,d]. For example, for the parent benzophenone system **4** examination of HOMO/LUMO coefficients (without regard to spin multiplicity) would indicate that electronic excitation (HOMO → LUMO) would result in considerable charge migration from the benzene ring with the CH_2OH substituent to the carbonyl group. This would enhance the basicity of the ketone oxygen making it easier to be protonated in the excited state. Moreover, there is enhanced depletion of charge at the *meta* position (with respect to the ketone; the ring carbon with the CH_2OH substituent) compared to the other positions, consistent with enhanced photoredox reactivity for this isomer.

Similar calculated results were observed for all of **6**–**10** (Fig. 4). In the case of xanthone **6**, there is substantial migration of charge from both benzene rings into the carbonyl group. Moreover, the electron density of the xanthene ring oxygen also migrates to the carbonyl group. This would result in a very basic carbonyl oxygen. In addition, there is substantial depletion of charge from the benzene ring carbon attached to the CH_2OH group. As well, the charge density of the C–H proton on the CH_2OH is also significantly depleted. Based on these simple calculated results, one would predict that xanthone **6** would be very reactive. In the case of fluorenone **7** (Fig. 4), the changes are similar but attenuated somewhat. For example, the depletion of charge at the benzene ring position attached to the CH_2OH is not as great. Indeed, there is more charge depletion at the other benzene ring positions for this compound although we have not studied these other isomers. These results for fluorenone **7** might indicate a less reactive system. As for all of **8**–**10** (shown only for **8** in Fig. 4), there is substantial migration of charge from the benzene ring with the CH_2OH substituent to the other benzene rings and to the carbonyl group. Moreover, the LUMO has bonding character between the carbons of the biphenyl ring system (seen for **9** and **10**), and antibonding character in the HOMO, giving these sys-

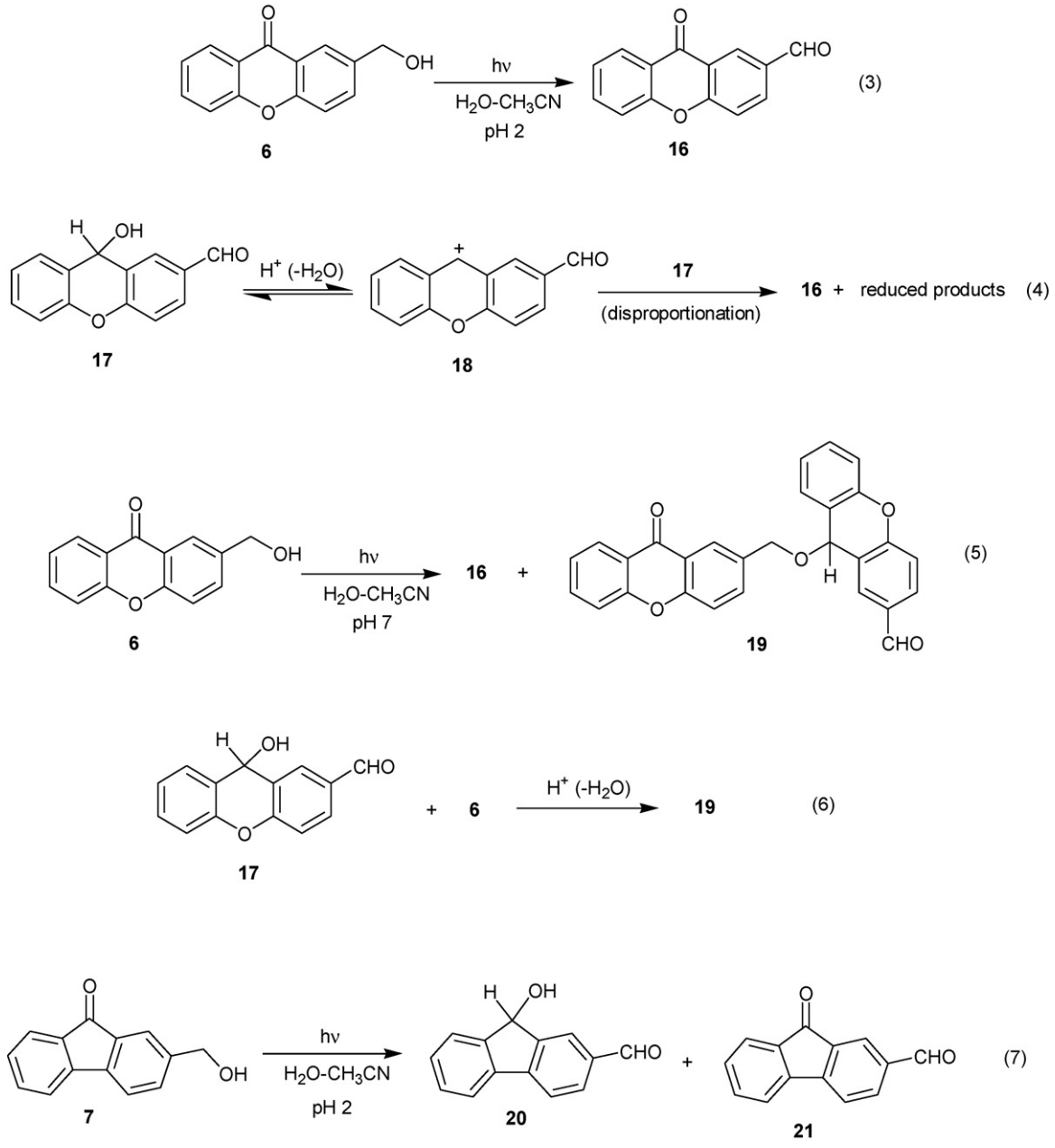

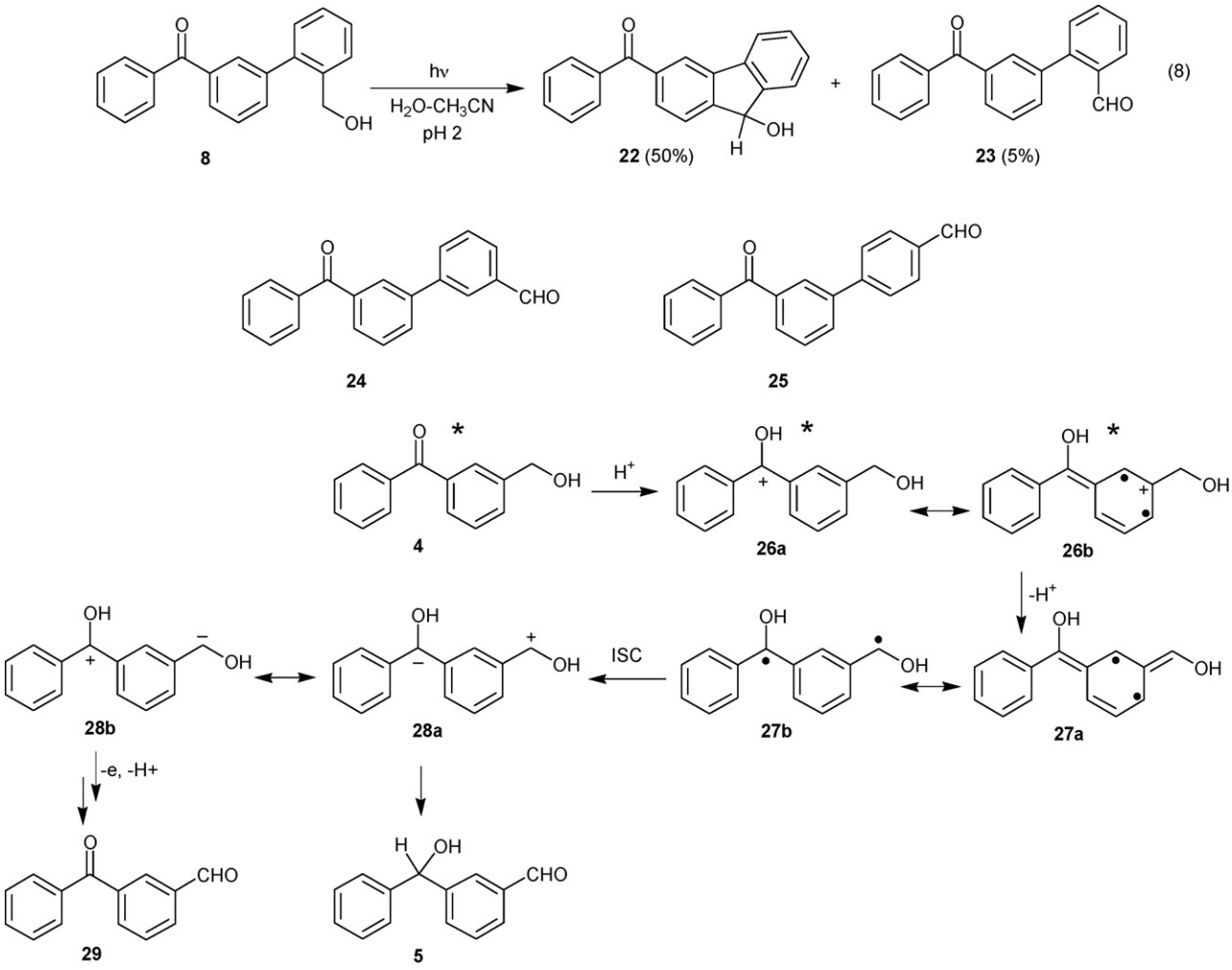

Scheme 2.

tems a tendency to planarize in the excited state hence allowing for better charge migration. One would predict that the calculated substantial migration of charge from the benzene ring containing the CH_2OH would make these systems quite reactive. The above simple predictions based on HOMO/LUMO calculations are confirmed qualitatively.

For reference, the proposed mechanism for the photoredox reaction of **4** is shown in Scheme 2 [6]. The data is consistent with triplet state reactivity although reaction via the singlet is not excluded. The first step of the mechanism involves protonation of the benzophenone ketone by acid. This step is analogous to the mechanism of acid catalyzed photohydration of benzophenone reported by Wirz and coworkers [5]. Protonation gives rise to an excited state carbocation **26a**,**b** that has its positive charge significantly delocalized to the *meta* position. The positive charge at the *meta* position of **26b** enhances the acidity of the benzylic C–H proton of the CH_2OH moiety significantly that it can be deprotonated by water to give the double enol **27a**,**b**. At this point, we visualize that the system will undergo a spin flip (ISC) to give the corresponding zwitterions. One of these is **28a** which would naturally lead to the observed formal redox product **5**. The other (**28b**) in which the charges are switched would lead to starting material **4**. However, exhaustive photolysis in D_2O failed to give detectable amounts of **4** that has a deuterium label at the C–H of the CH_2OH group, although of course we detected quantitative deuterium label at the benzhydrol C–H position of product **5**, as expected based on the zwitterionic structure of **28a**. The question arises as to the what are the pathways for reaction of **28b** if simple return to substrate is not one of them. Zwitterion **28b** is formally an α-hydroxycarbanion. We have studied the chemistry of members of these elusive species via photochemical generation [11] and found that their major pathway of reaction is disproportionation, that is via formal loss of an electron and a proton, to give the corresponding carbonyl radical anion, which upon workup in the presence of air, gives rise to what is formally an oxidized product (aldehyde or ketone). This finding is consistent with theoretical calculations that show that the simple $^{-}CH_2OH$ anion is unstable with respect to the corresponding radical [12] (formal oxidation), which is formally obtained by loss of an electron. Thus one of competing pathways for reaction in these formal intramolecular redox reactions is simple oxidation of the alcohol, via the α-hydroxycarbanion **28b**, eventhough it may appear to arise via residual reaction with dissolved oxygen. This simple oxidation pathway competes with or becomes the only observed pathway in the substrates studied in this work.

Based on the above calculations and proposed mechanism for the parent substrate **4**, a working mechanism for reaction of xanthone **6** is proposed as follows. This compound was found to be reactive in neutral solution (∼pH 7), the first system to display this sort of photoredox reactivity except for the anthraquinones [6a,f]. Reaction in pH 7 would indicate that the excited state is sufficiently basic to be protonated by water, or more likely protonated in concert with deprotonation of the benzylic proton of the

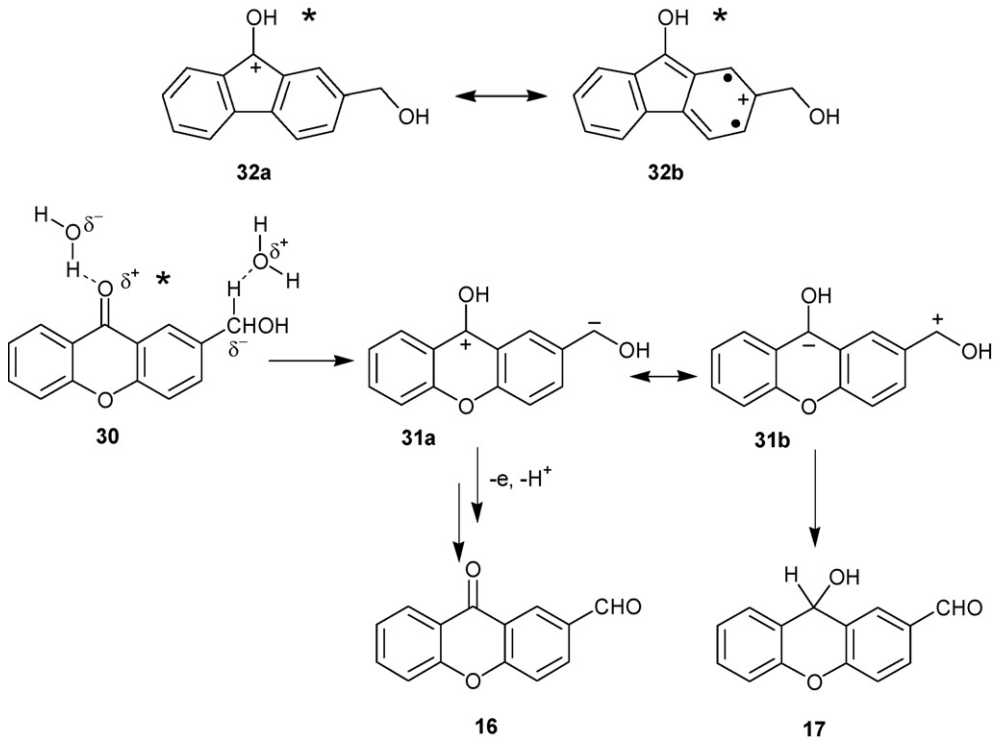

Scheme 3.

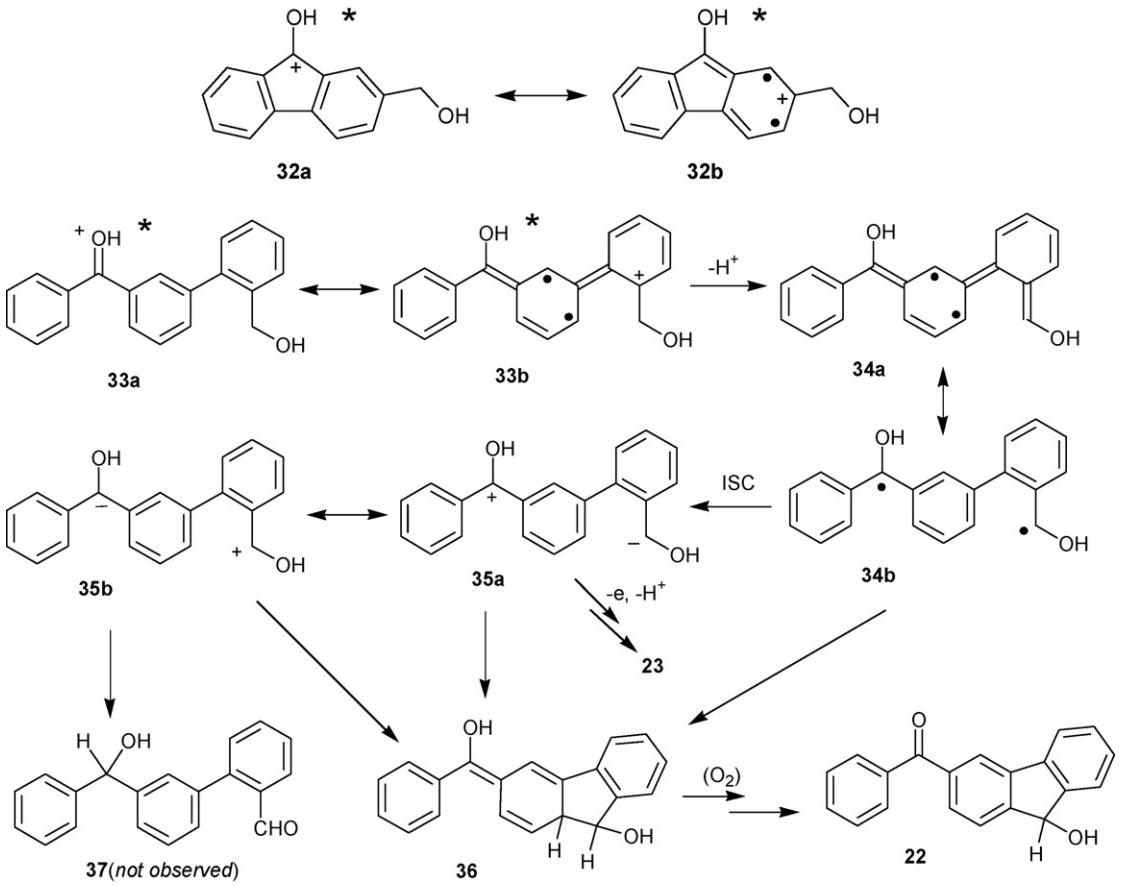

Scheme 4.

CH_2OH group, as shown in Scheme 3. After ISC, this gives rise to the two zwitterionic forms **31a**,**b**. The formal intramolecular redox product is obtained via **31b** and the oxidized product from **31a**. In acidic medium, direct protonation to give a discreet cation is possible, as proposed for **4**. However, since **17** is unstable thermally in acid, product studies in these pHs are more difficult to interpret.

HOMO/LUMO calculations have already suggested that fluorenone **7** might be an intrinsically less reactive system. This was indeed confirmed. However, extended photolysis in acid did result in formation of the redox product **20** along with the now expected **21**. An additional reason for the low reactivity of **7** is found in the nature of the cation upon protonation of the carbonyl oxygen (in the excited state). This initially gives rise to fluorenyl cation **32a**. In order for reaction to proceed, a significant fraction of the positive charge must reside at the *meta* ring position as shown in structure **32b**. We have shown in past work on the photosolvolysis of 9-fluorenol derivatives [13] that cations of the type **32a** are particularly favourable in the excited state and hence delocalization to the benzene positions might not be significant. This is an additional factor that may be responsible for the very low reactivity exhibited by the fluorenone system.

The best example of a "clean" photoredox chemistry in the systems studied in this work was observed for the *ortho* substituted biphenyl system **8**. Based on HOMO/LUMO calculations, all of **8**–**10** are anticipated to be reactive. This was indeed the case. However, the *ortho* substitution of the CH_2OH turns out to be essential for steering the mechanism to one resembling a redox reaction the most. Thus, protonation of the benzophenone ketone of **8** would lead to cations **33a**,**b**. Deprotonation of the benzylic C–H proton of the CH_2OH group would lead to **34a**,**b**. ISC would lead to the zwitterionic forms **35a**,**b**. Because of the location of the CH_2OH moiety, all of **34a**,**b** and **35a**,**b** can undergo simple aromatic substitution to give **36**! Indeed, this is apparently the major channel, in addition to a minor channel in the formation of **23** via **35a**. However, the simple formal redox product **37** was not observed, which in light of the facility of the ring closure pathway to form **38** does not seem surprising. Enol **36** would be expected to undergo fast ketonization (in acid), resulting in a dihydrobenzene which would not be isolable. Thus, upon workup (in air), only **22** was observed from this pathway. The *meta* and *para* isomers **9** and **10** would be expected to react via protonation followed by C–H deprotonation of the C–H proton of the CH_2OH group as shown in Scheme 4 for **8**. However, the crucial difference is that these isomers cannot undergo cyclization; in these systems, we see only the formal oxidized aldehyde products **24** and **25** in what appears to be an "aborted" redox process. We do not currently understand the reasons why these isomers do not proceed to products similar to **37** although such a pathway itself would be rather incredible if actually observed.

4. Conclusions

We have shown that a variety of suitably designed aromatic ketones undergo acid catalyzed formal photoredox chemistry indicating that the reaction is reasonably general. However, the redox products are sometimes not easily isolable or are diverted to form related products. There is clear indication that the photoredox chemistry of the benzophenone can be induced to more distal locations in the extended biphenyl systems. However, the location of the hydroxymethyl substituent's position on the new phenyl ring plays a pivotal role in the photobehaviour: only the *ortho*-substituted compound gave evidence of an intramolecular photoredox reaction, while the *meta*- and *para*-substituted compounds primarily exhibited photobehaviour that can be interpreted as indicative of an "aborted" intramolecular redox process. Overall, the added complexities observed in the system studied make them less useful compared to the "parent" benzophenone system.

Acknowledgment

Support of this research by NSERC (Canada) and the University of Victoria is gratefully acknowledged.

References

[1] G. Ciamician, P. Silber, Chem. Ber. 33 (1900) 2911.
[2] G.S. Hammond, W.M. Moore, J. Am. Chem. Soc. 81 (1959) 6334.
[3] W.M. Moore, G.S. Hammond, R.P. Foss, J. Am. Chem. Soc. 83 (1962) 2789.
[4] M.B. Ledger, G. Porter, J. Chem. Soc., Faraday Trans. 1 68 (1972) 539.
[5] M. Ramseier, P. Senn, J. Wirz, J. Phys. Chem. A 107 (2003) 3305.
[6] (a) M. Lukeman, M. Xu, P. Wan, J. Chem. Soc., Chem. Commun. (2002) 136;
(b) L.A. Huck, P. Wan, Org. Lett. 6 (2004) 1797;
(c) D. Mitchell, M. Lukeman, D. Lehnherr, P. Wan, Org. Lett. 7 (2005) 3387;
(d) N. Basaric, D. Mitchell, P. Wan, Can. J. Chem. 85 (2007) 561;
(e) Y. Hou, P. Wan, Can. J. Chem. 85 (2007) 1023;
(f) Y. Hou, P. Wan, Photochem. Photobiol. Sci. 7 (2008) 588.
[7] M. Eckstein, H. Marona, Polish J. Chem. 54 (1980) 1281.
[8] N.M. Yoon, C.S. Pak, H.C. Brown, S. Krishnamurthy, T.P. Stocky, J. Org. Chem. 38 (1973) 2786.
[9] P.J. Bullock, D.J. Byron, D.J. Harwood, R.C. Wilson, A.M. Woodward, J. Chem. Soc., Perkin Trans. II (1984) 2121.
[10] P. Wan, K. Yates, M.K. Boyd, J. Org. Chem. 50 (1985) 2881.
[11] J. Morrison, P. Wan, J.E.T. Corrie, V.R.N. Munasinghe, Can. J. Chem. 81 (2003) 586.
[12] K.M. Downard, J.C. Sheldon, J.H. Bowie, D.E. Lewis, R.N. Hayes, J. Am. Chem. Soc. 111 (1989) 8112.
[13] P. Wan, E. Krogh, J. Am. Chem. Soc. 111 (1989) 4487.